The 'Trinity' helix: Synthesis and structural characterisation of a C_3-symmetric tris-bidentate ligand and its coordination to Ag(I).

Brian Conerney, Paul Jensen, Paul E. Kruger* and Conchúir MacGloinn
Department of Chemistry, Trinity College, Dublin 2, Ireland.
E-mail: paul.kruger@tcd.ie

Electronic Supplementary Information

Figure ESI 1: Crystal structure of L. H-atoms and toluene molecule removed for clarity.

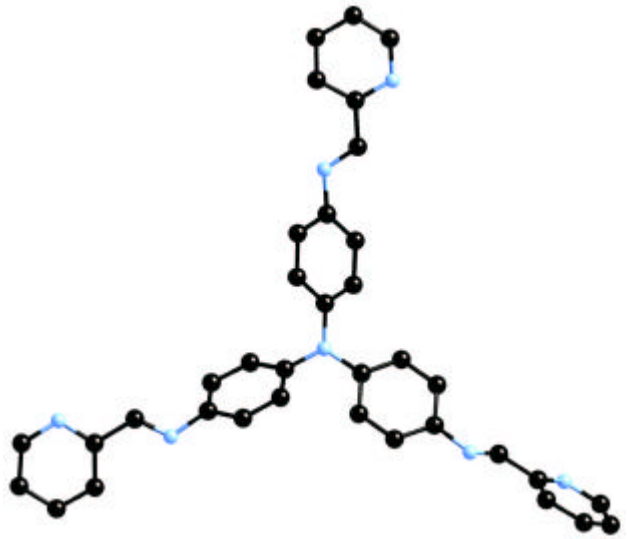

Figure ESI 2: Crystal packing diagrams of L.

The ligand forms an elaborate 3D H-bonded network involving at least three different modes of interaction as described below. Additional 'weaker' interactions (C-H···π type) are omitted here and will be described in a subsequent publication.

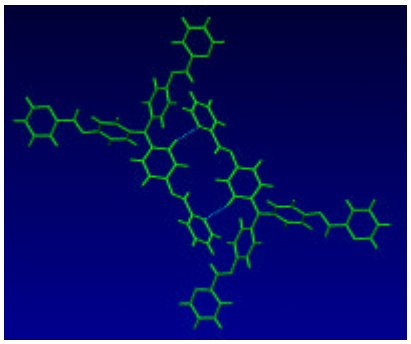

A H-bond interaction between a central aromatic ring hydrogen to an adjacent pyridyl nitrogen links two arms:
H6c···N3c 2.580 Å, < C6c–H6c···N3c 155°; symmetry code 1 - x, 1 - y, 1 -z).

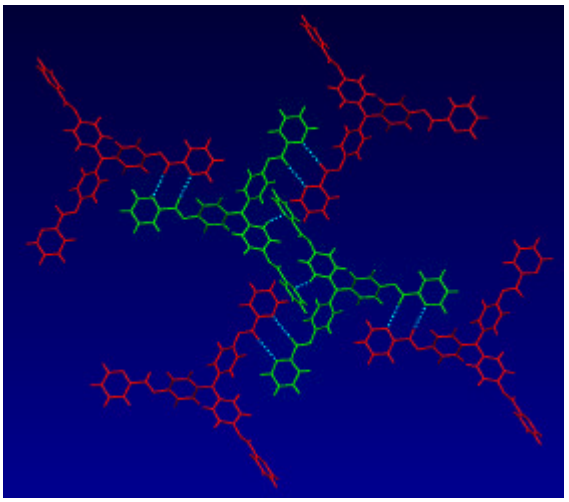

H-bonding between an imino hydrogen and pyridyl nitrogen links these units together forming a 2D sheet:
H7b···N3b 2.678 Å, < C7b–H7b···N3b 163°; symmetry code 1 - x, 1 - y, 1 -z)

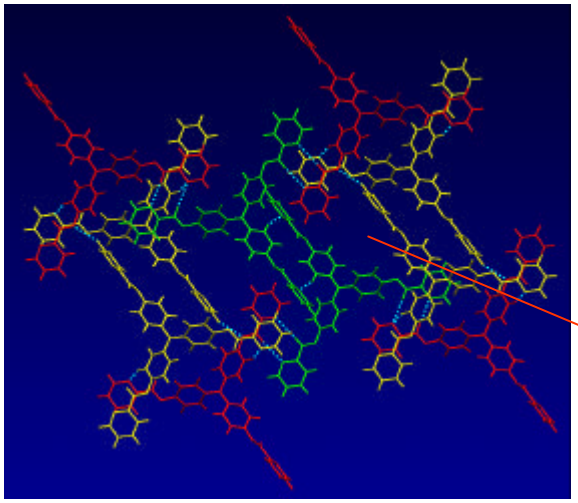

A H-bond interaction between a central aromatic ring hydrogen to an adjacent pyridyl nitrogen links the sheets into 3D: H3a···N3b 2.611 Å, < C3a–H3a···N3b 144°; symmetry code - x, - y, 2 -z).

Disordered toluene molecules (not shown) occupy channels.

Figures generated with Mercury 1.1.2, CCDC: www.ccdc.cam.ac.uk/mercury/

Figure ESI 3: Electrospray Mass Spectrum of $[Ag_3L_2](PF_6)_3$

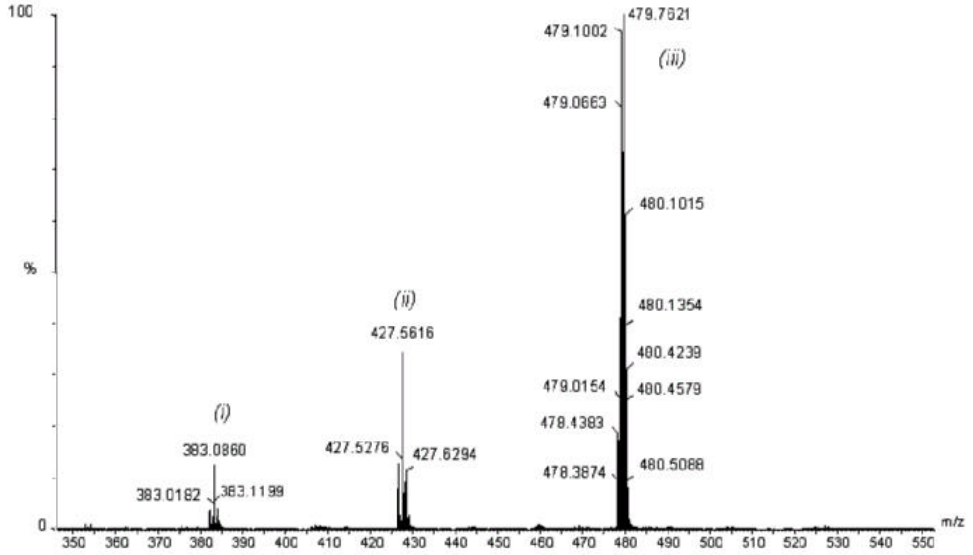

(a) The ESMS of $[Ag_3L_2](PF_6)_3$ from MeCN/$CHCl_3$ solutions showing the parent ion, $[Ag_3L_2]^{3+}$ (*iii*), centred around *m/z* 479.762. Note the absence of peaks accounting for any other M:L stoichiometry. Peaks (*i*) and (*ii*) are fragmentation products.

Peak (*i*) at 383.08 *m/z* is assigned to fragmentation product resulting on loss of a pyridyl unit generating L′, where L′ = $C_{30}H_{24}N_6$, to give $[Ag_2(MeCN)_2L']^{2+}$. (Calc. *m/z* for $[Ag_2C_{34}H_{30}N_8]^{2+}$ = 383.02)

Peak (*ii*) at 427.56 *m/z* is assigned to the fragmentation product that results on loss of L and Ag(I) to give $[Ag_2(MeCN)_2L]^{2+}$. (Calc. *m/z* for $[Ag_2C_{40}H_{33}N_9]^{2+}$ = 427.75)

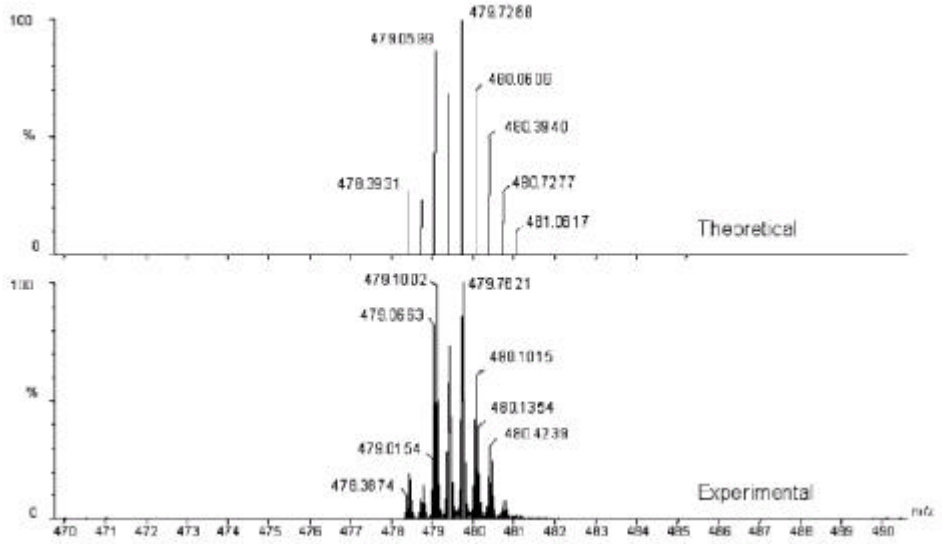

(b) The theoretical mass and isotopic peak pattern (*top*) compared with the experimentally found mass and isotopic peak pattern (*bottom*) for $[Ag_3L_2]^{3+}$ *i.e.* $[Ag_3C_{72}H_{54}N_{14}]^{3+}$

Figure ESI 4: **Molecular models of (a) *rac*-$[Ag_3L_2]^{3+}$ and (b) *meso*-$[Ag_3L_2]^{3+}$**

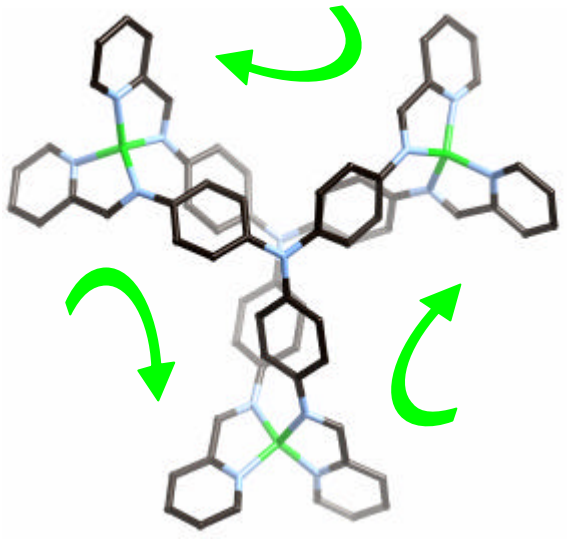

(a) *rac*-$[Ag_3L_2]^{3+}$ showing the helical nature of the complex. Note how *each* ligand 'arm' crosses over the Ag-Ag axis. The Λ-enantiomer is shown.

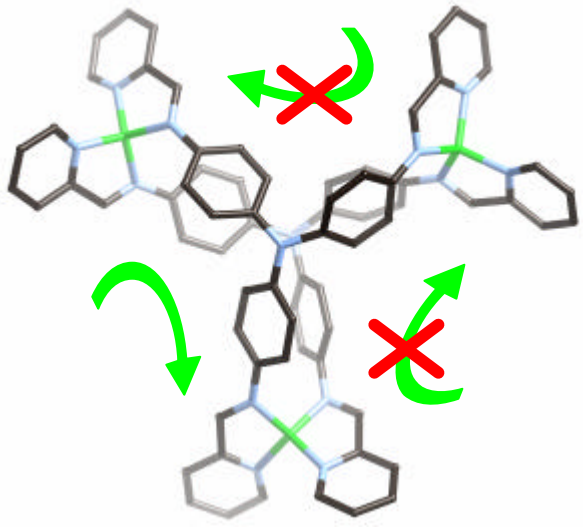

(b) *meso*-$[Ag_3L_2]^{3+}$ showing both the helical nature of the complex as indicated by the arrow, and the non-helical nature as indicated by the crossed arrows. Note how *only* one ligand 'arm' (from each ligand) crosses over the Ag-Ag axis. Irrespectively, the '*meso*'- isomer must always retain a helical strand.

The models were generated using ISIS Draw version 2.1.1 (MDL Information Systems) and the geometries optimised using Hyperchem version 7.0 (Hypercube Inc.).